Proton-proton correlations: Determination of the source size and lifetime from deep inelastic collisions of ^{58}Ni + ^{58}Ni at 15 MeV/nucleon

M. Korolija
Physics Division, Oak Ridge National Laboratory, Oak Ridge, Tennessee 37830
and Ruder Boskovic Institute, 41001 Zagreb, Croatia

D. Shapira and J. Gomez del Campo
Physics Division, Oak Ridge National Laboratory, Oak Ridge, Tennessee 37830

E. Chavez
Instituto de Fisica, Universidad Nacional Autónoma de México, A.P. 20-364, 01000 Mexico D.F., Mexico
and Physics Division, Oak Ridge National Laboratory, Oak Ridge, Tennessee 37830

N. Cindro
Ruder Boskovic Institute, 41001 Zagreb, Croatia
(Received 9 July 1993)

Triple (p-p-fragment) coincidences from the ^{58}Ni + ^{58}Ni reaction at 850 MeV have been measured. By detecting the source of the emitted particles we were able to study the directional dependence of the p-p correlation function. From this dependence both the source size (r_0) and the particle emission time (τ) have been extracted. The extracted p-p correlation functions could be fitted with source size and lifetime in the range of $3.3^{+1.3}_{-0.7}$ fm and $3.2^{+1.3}_{-2.2}\times 10^{-22}$ s, respectively.

PACS number(s): 25.70.Pq, 21.65.+f

I. INTRODUCTION

The technique of measuring light particle correlations offers a unique method to extract characteristic spatial and temporal information about the zone where these particles are generated [1–6]. To obtain such information various pairs of light particles have been employed in correlation studies [7–13]. Generally speaking, an enhancement in the light particle correlations occurs either when the two emitted light particles are in close proximity [14–15] or when they are emitted as a preformed complex [17–19].

Proton-proton (in further text referred to as p-p) pairs have been used quite frequently in correlation studies, primarily because protons are relatively east to identify. Furthermore, in many instances, e.g., for low emission temperatures, the probability of emission of preformed *He^2 fragments is small compared to that of the emission of two protons with nearly equal momenta [17,20]. In the latter case, the enhancement in the p-p correlation function is due to the p-p final-state interaction. In particular, there is a strong enhancement in the p-p correlation function at $\Delta p = 20$ MeV/c ($\Delta p = \frac{1}{2})|\mathbf{p}_2 - \mathbf{p}_1|$, where $\mathbf{p}_1$ and $\mathbf{p}_2$ are, respectively, the laboratory momenta of the two protons). This enhancement comes as a result of the attractive nuclear force dominating the combined action of the repulsive Coulomb force and the effects of the Fermi statistics [14].

In p-p final-state interaction models [14–16], two parameters determine the p-p correlation function. These are the source size r_0 and the product of the relative velocity and the emission time, $\mathbf{v}_{\rm rel}\tau$ [$\mathbf{v}_{\rm rel}$ is the velocity of the p-p pair ($\mathbf{v}_{pp}$), relative to the source velocity ($\mathbf{v}_0$), i.e., $\mathbf{v}_{\rm rel} = \mathbf{v}_{pp} - \mathbf{v}_0$]. In order to determine the two quantities, r_0 and τ, one needs to measure (or else specify) the relative velocity $v_{\rm rel}$. To obtain this information, a new generation of light-particle coincidence experiments is needed in which light particles are measured in coincidence with heavy fragments. These experiments aim at the determination of the source of the emitted light particles through their correlation. Notice, however, that even when $v_{\rm rel}$ is known, there is still an ambiguity in the determination of r_0 and τ, if these parameters are not deduced from the simultaneous fit to both the perpendicular and the longitudinal p-p correlation function. In earlier papers [5,21], studies using the directional dependence of the p-p correlation function were attempted but in these cases there was no experimental information about the velocity or nature of the emitting source.

In this paper we report on measurements of p-p-fragment triple coincidences from deep inelastic collisions of ^{58}Ni + ^{58}Ni at 15 MeV/nucleon. As noted in Ref. [14], for the same values of the parameters r_0 and τ, there is a difference in the shape of the p-p correlation function when (a) $\Delta\mathbf{p}$ is perpendicular to $\mathbf{v}_{\rm rel}$ and (b) $\Delta\mathbf{p}$ is parallel to $\mathbf{v}_{\rm rel}$. The parameters r_0 and τ were deduced from this difference in the p-p correlation functions by requiring a simultaneous fit to both subsets of the p-p correlation function. The values obtained for these parameters are found to be consistent with those obtained in an earlier analysis of the same reaction [22]. Thus, the analysis presented in this paper differs from that presented in Ref. [22] where the parameters r_0 and τ were determined from a $v_{\rm rel}$ dependence of the p-p correlation function.

This paper is organized as follows. The description of the experimental layout is given in Sec. II. In Sec. III, we discuss the p-p correlation analysis and briefly describe the experimental problems related to the construction of the background yield. We continue the background construction discussion in Sec. IV, where we also describe the event mixing procedure in detail. In Sec. V we compare our results with theoretical predictions. This section also contains the discussion of our results. Finally, in Sec. VI we summarize the obtained results.

II. EXPERIMENTAL LAYOUT

The experiment was performed with an 850 MeV ^{58}Ni beam produced by the coupled accelerator facility at the ORNL Holifield Heavy Ion Research Facility. The areal density of the ^{58}Ni target was 1 mg/cm^2. Triple p-p-fragment coincidences were measured using the heavy-ion–light-ion (HILI) detection system [23]. Figure 1 shows a schematic view of the experimental layout.

The charge and the energy of the heavy fragment were obtained from the position sensitive ionization chamber, while the direction of the heavy fragment was obtained by combining the signals from the ionization chamber and a parallel plate avalanche counter (PPAC) with multiwire position read-out. The heavy fragments used in the analysis were in the charge range of $21<Z<26$.

Light charged particles and light fragments were measured using an array of 96 ΔE-E phoswich scintillator detectors [24]. The energy calibration for protons was performed by measuring the elastic scattering of the ^{58}Ni beam from protons in a polypropylene target at two different beam energies. The average angular resolution of the light-particle detectors was about 2°. In the analysis, the azimuthal and polar angles of each of these detectors were randomized over the detector area. The maximum detection polar angle was 22°.

III. CORRELATION ANALYSIS

The correlation function R is defined as the normalized ratio of the two-particle coincidence cross section to the product of the single-particle cross sections, i.e.,

$$R(\mathbf{p}_1,\mathbf{p}_2)+1=\frac{\dfrac{1}{\sigma_{\text{coinc.}}}\dfrac{d^2\sigma_{\text{coinc.}}}{d\mathbf{p}_1 d\mathbf{p}_2}}{\left[\dfrac{1}{\sigma_{\text{singl.}}}\dfrac{d\sigma_{\text{singl.}}}{d\mathbf{p}_1}\right]\left[\dfrac{1}{\sigma_{\text{singl.}}}\dfrac{d\sigma_{\text{singl.}}}{d\mathbf{p}_2}\right]} . \quad (1)$$

In Eq. (1), the two-particle coincidence cross section contains both the correlated and the uncorrelated particle pairs, while the product of the single-particle cross sections is a function of uncorrelated particles only. The asymptotic behavior of the function $R(\mathbf{p}_1,\mathbf{p}_2)$ is assumed to be such, that at large Δp all two-particle correlation effects vanish, i.e., $R(\mathbf{p}_1,\mathbf{p}_2)=0$ and the two-particle coincidence cross section is equal to the product of the single-particle cross sections.

The determination of $R(\mathbf{p}_1,\mathbf{p}_2)$ from the experimental data is often complicated by the various experimental biases and conditions which need to be taken into account. For example, the measured single-particle and coincidence yields may not originate from the same source, i.e., result from the same mechanism. This assumption is, however, implicit in Eq. (1). To avoid this problem, a different approach to the construction of the background yield has been suggested. In this approach, the background yield is constructed from the two-particle coincidence yield by mixing particles from different coincidence events [25,26] rather than constructing it from

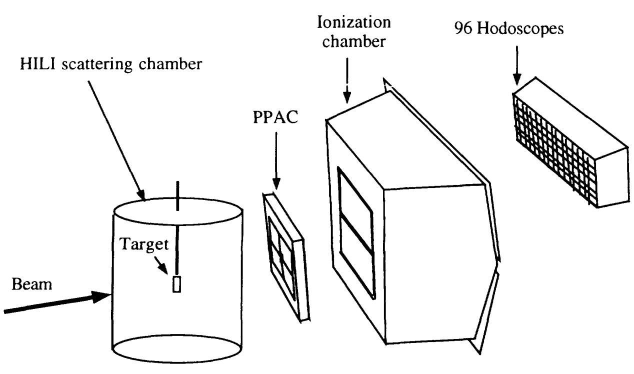

FIG. 1. Schematic view of the HILI (heavy-ion-light-ion) detection system.

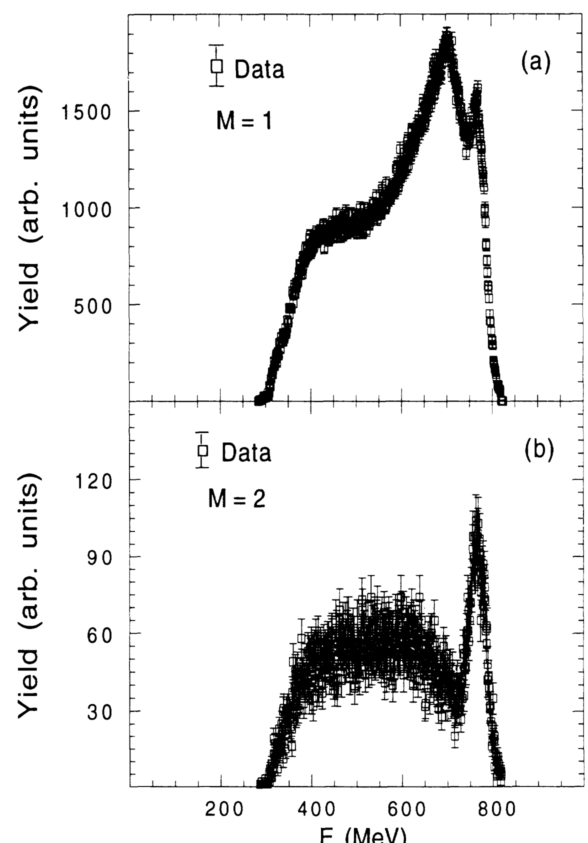

FIG. 2. Heavy fragment energy spectra for (a) proton multiplicity $M=1$ and (b) $M=2$. The detected heavy fragments are in the charge range of $21<Z<26$.

the product of the single-particle yields [27,28]. By using the mixing method, one hopes that all effects, except the genuine two-particle correlations, will be contained in both the numerator and the denominator of Eq. (1) and, therefore, effectively cancel out.

A comparison between the two different background construction schemes was recently done for the $^{14}N+^{27}Al$ reaction at 75 MeV/nucleon [29]. The two different techniques were found to yield virtually identical results. This, however, need not be generally true; it is probably correct for the $^{14}N+^{27}Al$ reaction at very high energies, where the complete breakup of the composite nuclear system into individual nucleons is probable, which is not the case for the reaction studied in this work. Figure 2 shows the fragment energy spectra in coincidence with protons of multiplicity 1 and 2; it is clear from the shape of the two spectra that the proton multiplicity serves as a reaction filter and that the single proton-fragment coincidences do not originate from the same process as the *p*-*p*-fragment coincidences.

Therefore, we have opted to use event mixing of triple coincidence data to get the background for our correlation studies. Because the *p*-*p* correlation function in our measurement is associated with exclusive *p*-*p*-fragment triple coincidences it will have to be written in a way that explicitly takes into account the presence of the heavy fragment, in addition to the two light particles. Equation (1) thus reads

$$R(\mathbf{p}_1,\mathbf{p}_2,\mathbf{p}_f)+1=C\frac{\sigma_{123}(\mathbf{p}_1,\mathbf{p}_2,\mathbf{p}_f)}{\Sigma_i\Sigma_j\sigma'_{123}(\mathbf{p}_{1,i},\mathbf{p}_{2,i},\mathbf{p}_{f,i};\mathbf{p}_{1,j},\mathbf{p}_{2,j},\mathbf{p}_{f,j})}\,, \tag{2}$$

where $\sigma_{123}(\mathbf{p}_1,\mathbf{p}_2,\mathbf{p}_f)$ is the measured yield of *p*-*p*-fragment coincidences consisting of protons (with momenta $\mathbf{p}_1$ and $\mathbf{p}_2$, respectively) and a fragment (with momentum $\mathbf{p}_f$). The fragment momentum $\mathbf{p}_f$ was determined from the measured fragment charge, energy, and polar and azimuthal angle distributions, with the fragment mass taken as the most probable mass obtained from a distribution calculated with the statistical evaporation code LILITA [30]. The background yield

$$\sigma'_{123}(\mathbf{p}_{1,i},\mathbf{p}_{2,i},\mathbf{p}_{f,i};\mathbf{p}_{1,j},\mathbf{p}_{2,j},\mathbf{p}_{f,j})$$

was constructed by mixing protons $\mathbf{p}_{1,i}$ and $\mathbf{p}_{2j}$ from events *i* and *j*, respectively. Note here that the structure of Eq. (2) is basically the same as that of Eq. (1), since the integration of Eq. (2) of $\mathbf{p}_f$ yields Eq. (1). Equation (2) is normalized to the theoretical $R(\mathbf{p}_1,\mathbf{p}_2)$ at large Δp through the normalization constant *C*.

IV. EVENT MIXING

This section deals with the Monte Carlo simulation procedure for the emission of uncorrelated proton pairs, effects of the final-state interaction between emitted protons, and a self-consistency test of the event mixing technique to assure the usage of this technique later on in the analysis of the experimental data.

In the Monte Carlo simulation procedure two protons are generated in the source rest frame. The momentum (p), theta (θ), and phi (ϕ) distributions associated with the two proton emission are given in Figs. 3(a)–3(c), respectively. These distributions were chosen as such to closely reflect the p, θ, and ϕ distributions acquired in the experiment. We proceed further by calculating the Δp distribution of uncorrelated proton pairs. This distribution will be compared with the (i) Δp distribution obtained by turning on the *p*-*p* final-state interaction and (ii) Δp distribution obtained by mixing events from (i). Obviously, in the case (i) the ratio of the Δp distributions obtained with and without *p*-*p* final-state interaction should

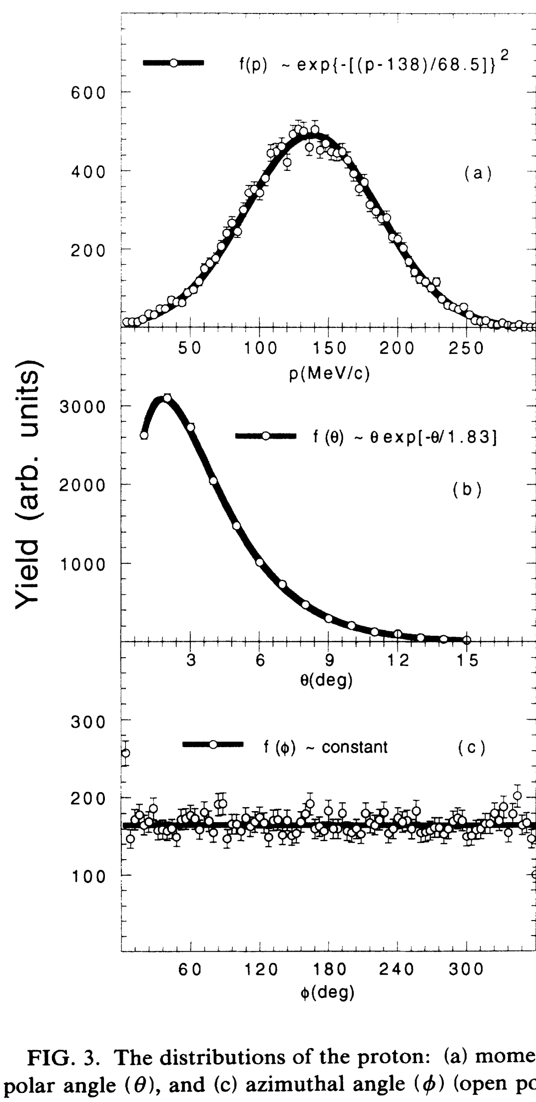

FIG. 3. The distributions of the proton: (a) momenta (p); (b) polar angle (θ), and (c) azimuthal angle (ϕ) (open points). The solid curves are parametrization used as input to the Monte Carlo simulation.

give us back the net effect of the p-p final-state interaction, i.e., the p-p correlation function R itself. In the case (ii), however, if the event mixing procedure works well, then the Δp distribution obtained by mixing events from (i), i.e., by mixing events of particles with correlations, should be identical to the Δp distribution of uncorrelated proton pairs. We now turn to the description of turning on the p-p final-state interaction between emitted uncorrelated proton pairs.

The final-state interaction between two protons is turned on assuming that the proton emission could be associated with a fixed source size r_0 and fixed emission time τ. Furthermore, for given values of the parameters r_0 and τ the proton pair correlation was weighted according to the calculated p-p correlation function R using the model of Ref. [14]. To obtain a correct weighting of the p-p final-state interaction a pool of 100 p-p correlation functions was used. The p-p correlation functions were calculated for a source size of $r_0=3$ fm and the values of the parameter $v_{\rm rel}\tau$ in the range of 0 fm $< v_{\rm rel}\tau <$ 12 fm, respectively. Note that this was necessary since although the parameter τ was fixed, the relative velocity $v_{\rm rel}$ is different for different events. To simplify the test procedure, the dependence of the p-p correlation function on the angle between $\mathbf{v}_{\rm rel}$ and $\Delta\mathbf{p}$ was not taken into account.

Figures 4(a) and 4(b) show the results of a self-consistency test of the event mixing technique for a source size of $r_0=3$ fm and two different values of the parameter τ, respectively. Full curves in Figs. 4(a) and 4(b) show the ratios R corresponding to the case where the p-p final-state interaction was turned on and off in the Monte Carlo calculation [case (i)]. On the other hand, open symbol in Figs. 4(a) and 4(b) show the ratios R obtained by dividing the Δp distribution with correlations by the same Δp distribution but obtained by mixing events [case (ii)]. As one can see from Fig. 4, the ratios R obtained by switching the p-p final-state interaction on and off in the Monte Carlo calculation (full curve) fits very well with the ratio R obtained by mixing events (open symbols).

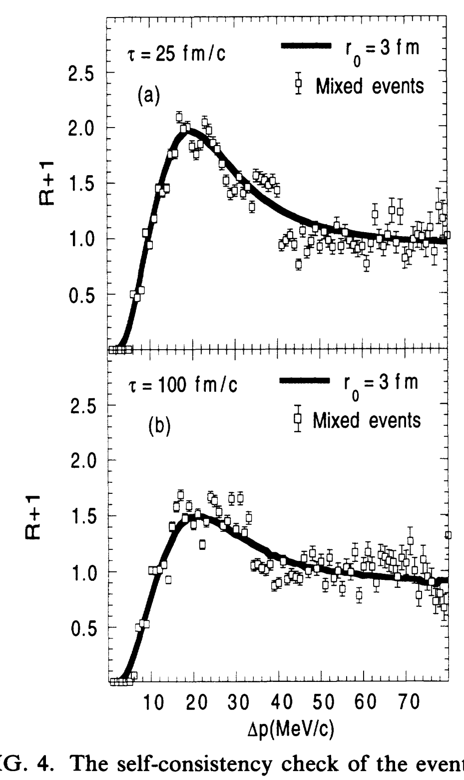

FIG. 4. The self-consistency check of the event mixing procedure. The full lines refer to the p-p correlation where the final-state interaction between two protons is calculated exactly, i.e., with weight according to the ratio r for a given event. Open symbols refer to the extraction of the p-p correlation function (from the same set of data) but going through a step of mixing events rather than calculating the ratio R exactly. In the test procedure, a source size of $r_0=3$ fm and a lifetime of (a) $\tau=25$ fm/c and (b) $\tau=100$ fm/c were used, respectively. In all calculations the source that emits particles was at rest.

V. RESULTS AND DISCUSSION

It is well known [14–16] that for nonvanishing characteristic emission time τ, the p-p correlation function depends on the both Δp and the angle between $\Delta\mathbf{p}$ and $\mathbf{v}_{\rm rel}$ ($\theta_{\rm rel}$). We explore this directional dependence of p-p correlation function in an attempt to deduce both parameters, r_0 and τ. To achieve this goal, the p-p correlation function was analyzed in two limiting cases (1) for small $\Delta p_\perp$ and (2) for small $\Delta p\|$. Ideally, one would like to impose tight constraints ($\Delta p_\perp$ or $\Delta p_\| = 0$) on the analyzed p-p correlation functions, but due to limited momentum resolution and the limited number of triple coincidence events, the above conditions were approximated with

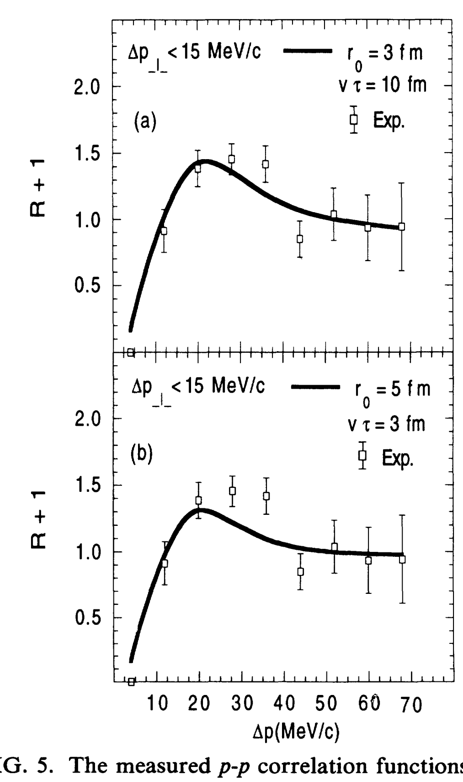

FIG. 5. The measured p-p correlation functions corresponding to the $\Delta p_\perp < 15$ MeV/c cut being imposed on the data. The solid lines show two different fits to the extracted p-p correlation function, respectively.

$\Delta p_{\perp}(\Delta p\|) < 15$ MeV/c.

The p-p correlation function obtained by imposing the $\Delta p\perp < 15$ MeV/c cut on the data is shown in Fig. 5 (open symbols). Figure 6 shows the same but for the $\Delta p_{\|} < 15$ MeV/c cut being imposed on the data. Solid lines in Figs. 5 and 6 show the calculated p-p correlation functions for two different sets of parameters calculated using the model from Ref. [14]. In calculating these these p-p correlation functions, the finite (angular) detector resolution was taken into account by averaging the model calculations over the same Δp bin size (8 MeV/c) as used in averaging the measured data. To ease the comparison between the measured p-p correlation functions and the model calculations so averaged, model calculations (i.e., points) were then jointed by a smooth curve (see Figs. 5 and 6). As one can see from Figs. 5 and 6, the p-p correlation functions could be described either with a set of parameters of $r_0=3$ fm $v_{\rm rel}\tau=10$ fm or with a set of $r_0=5$ fm, $v_{\rm rel}\tau=3$ fm. To check the sensitivity of the extracted p-p correlation functions on the parameters r_0 and $v_{\rm rel}\tau$ a χ^2 was calculated for the model and the extracted p-p correlation functions using the following expression

$$X^2=\sum_i \left[\frac{R_i^{\rm exp}-R_i^{\rm th}}{\Delta R_i^{\rm exp}} \right]^2 , \tag{3}$$

where $R_i^{\rm exp}$ and $R_i^{\rm th}$ are the experimental and calculated p-p correlation function. The extracted p-p correlation functions and $\Delta R_i^{\rm exp}$ are uncertainties in the experimentally extracted p-p correlation functions are normalized to 1 at large Δp where no correlation is assumed as shown in Figs. 5 and 6. Once the normalization constant C [see Eq. (2)] was determined it was kept fixed throughout the whole analysis.

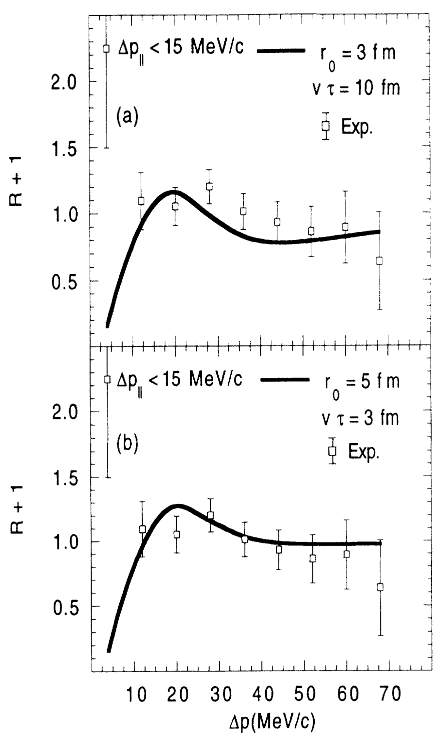

FIG. 6. Same as Fig. 5 but for the $\Delta p_{\|} < 15$ MeV/c.

A contour plot representation of the χ^2 values is shown in Fig. 7 for a $\Delta p_{\perp} < 15$ MeV/c cut on the data. Figure 8 shows the same for the $\Delta p_{\|} < 15$ MeV/c cut being imposed on the data. The contour plots shown in Figs. 7 and 8 are obtained by calculating the X^2 in the range of 2.6 fm $< r_0 < 5$ fm and 0 fm $< v_{\rm rel}\tau < 12$ fm in steps of $\Delta r_0 = 0.4$ fm and $\Delta(v_{\rm rel}\tau)=3$ fm, respectively. In calculating the χ^2 values the first point of the extracted p-p correlation functions, which was below 10 MeV/c, was left out from the calculations.

A glance at Fig. 7 ($\Delta p_{\perp} < 15$ MeV/c reveals that the calculated X^2 values show a minimum at $r_0 \sim 3.5$ fm and $v_{\rm rel}\tau \sim 9$ fm. A 25% variation in the calculated X^2 around this minimum is associated with a band of correlated r_0 and $v_{\rm rel}\tau$ values where a larger value for the source size r_0 is associated with a smaller value for the parameter $v_{\rm rel}\tau$ and vice versa. On the other hand, the calculated X^2 values from Fig. 8 ($\Delta p_{\|} < 15$ MeV/c), show a shallower minimum at $r_0 \sim 4.5$ fm and $v_{\rm rel}\tau \sim 6$ fm. A 25% variation in the calculated X^2 around this minimum includes a wider band of correlated r_0 and $v_{\rm rel}\tau$ values. As was already clear from Fig. 6, relatively large error bars associated with the p-p correlation function obtained by imposing the $\Delta p_{\|} < 15$ MeV/c cut on the data, prevents us from obtaining better steepness of the calculated X^2 values. Therefore, in what follows, we rely on the X^2 analysis from Fig. 7, i.e., we take the ranges of $r_0 = 3.3^{+1.3}_{-0.7}$ fm (Gaussian density) and $v_{\rm rel}\tau = 9^{+3}_{-1}$ fm as the final values for the extracted parameters r_0 and $v_{\rm rel}\tau$. Assuming a uniform density distribution as a source density distribution we obtain $r_0 = 5.2^{+2.0}_{-1.1}$ fm. This value for the source size is quite reasonable since deep inelastic fragments are about the size.

The $\theta_{\rm rel}$ distributions obtained by applying the $\Delta p_{\perp}$ ($\Delta p_{\|}$) < 15 MeV/c cut on the data is shown in Fig. 9(a) [9(b)]. In fact, these two figures show the directional cuts used in the data analysis. Figure 10(a) shows the $v_{\rm rel}$ distribution obtained by imposing the $\Delta p_{\perp} < 15$ MeV/c

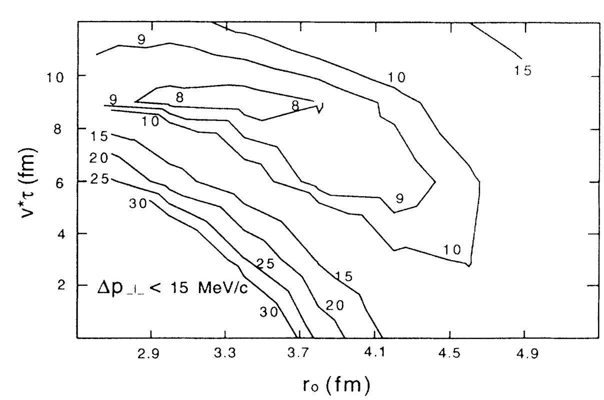

FIG. 7. Contour plot representation of the χ^2 values obtained by using Eq. (3) for $\Delta p_{\perp} < 15$ MeV/c cut being imposed on the data. The χ^2 values are given as a function of the fit parameters r_0 and $v_{\rm rel}\tau$, respectively.

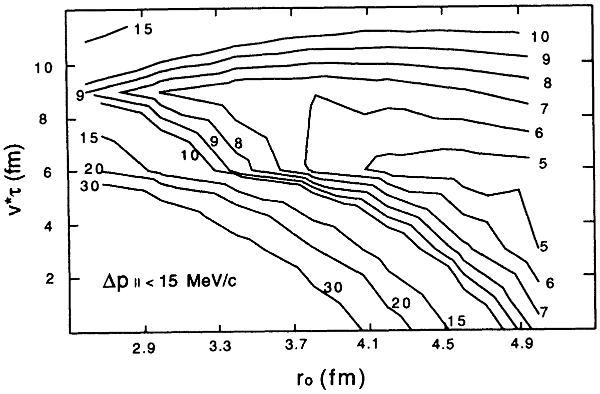

FIG. 8. Same as Fig. 9 but for the $\Delta p_{\parallel} < 15$ MeV/c.

cut on the data. Figure 10(b) shows the same but for the $\Delta p_{\parallel} < 15$ MeV/c cut being imposed on the data. These distributions will be used now to extract the range of emission times τ from corresponding to the p-p correlation functions shown in Figs. 5 and 6, respectively.

The value for the parameter τ was obtained by specifying the most probable v_{rel} from the v_{rel} distributions shown in Figs. 10(a) and 10(b). A Gaussian fit to these v_{rel} distributions yields for the most probable v_{rel} velocity a value of $\langle v_{rel}/c \rangle = 0.11$. Combining this information with the knowledge that the variation of the parameters r_0 and $v_{rel}\tau$ in the ranges of 2.6 fm $< r_0 < 4.6$ fm and 3 fm $< v_{rel}\tau < 12$ fm still gives an acceptable fit to the extracted p-p correlation, one obtains for the parameter τ an average value of $(3.2 \pm 1.5) \times 10^{-22}$ s. This value for the

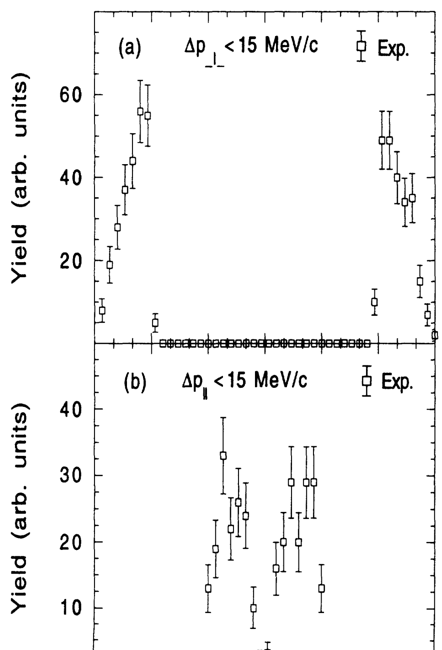

FIG. 9. Distributions of θ_{rel}, the angle between $\mathbf{\Delta p}$ and $\mathbf{v}_{rel}$, obtained by applying the (a) $\Delta p_{\perp} < 15$ MeV/c and (b) $\Delta p_{\parallel} < 15$ MeV/c cuts on the data.

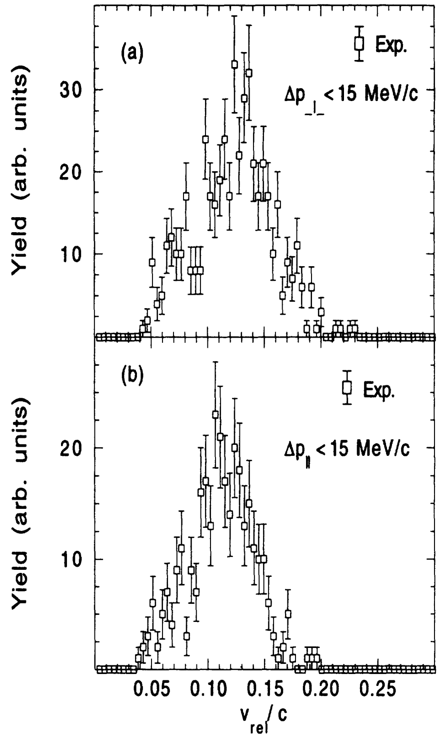

FIG. 10. Distributions of v_{rel} obtained by applying the (a) $\Delta p_{\perp} < 15$ MeV/c and (b) $\Delta p_{\parallel} < 15$ MeV/c cuts on the data.

emission time τ fits well within the recently deduced nuclear emission times of highly excited composite nuclei [3,11].

VI. CONCLUSION

Triple p-p-fragment correlation's from the deep inelastic ^{58}Ni+^{58}Ni collision have been measured at 15 MeV/nucleon. This provides information about the source velocity of the emitted light particles relative to the p-p c.m. The knowledge of this velocity was necessary to extract both the source size r_0 and its lifetime τ from a directional (θ_{rel}) dependence of the p-p correlation function.

The source size r_0 and the lifetime τ have been determined by extracting the p-p correlation function in two limiting cases. In one case the perpendicular component of $\mathbf{\Delta p}$ was small, while in the other case the longitudinal component of $\mathbf{\Delta p}$ was small. (The longitudinal and the perpendicular components of $\mathbf{\Delta p}$ are defined with respect to the relative direction between the heavy fragment and p-p c.m. velocities). By imposing these directional cuts on the data, we were able to fit the p-p correlation function with a set of source sizes in the range of $r_0 = 3.3^{+1.3}_{-0.7}$ fm (Gaussian density) and light-particle emission times in the range of $\tau = 3.2^{+1.3}_{-2.2} \times 10^{-22}$ s, respectively.

While our triple coincidence data allowed us to resolve some competing effects affecting the p-p correlations, it is clear that greater statistics and better momentum resolution are needed to improve the sensitivity of the extracted p-p correlation functions on source parameters. In a previous publication [22] we have used cuts on the p-p c.m. velocity to arrive at similar results; the presently available statistics do not allow a simultaneous application of both the relative velocity and directional cuts. A second level trigger has been implemented in the experimental setup which allows a 10-fold improvement in the rate at which triple and higher coincidence level data can be accumulated. Improvements in detector granularity for better relative momentum resolution data are also underway.

ACKNOWLEDGMENTS

The authors are indebted to H. J. Kim, J. Y. Shea, and K. Teh for their help in preparing the experiment and running it and T.C. Awes for simulating discussions. This work was supported by US-DOE/IRB Contract No. JF 939. One of the authors (N.C.) gratefully acknowledges the hospitality of the Joint Institute for Heavy Ion Research, HHIRF, Oak Ridge, TN 37831. ORNL is managed by Martin Marietta Energy Systems, Inc., under Contract No. DE-AC05-84OR21400 with the U.S. Department of Energy.

[1] D. H. Boal, C. K. Gelbke, and B. K. Jennings, Rev. Mod. Phys. **62**, 553 (1990), and references therein.
[2] W. G. Gong, C. K. Gelbke, N. Carlin, R. T. de Souza, Y. D. Kim, W. G. Lynch, T. Murakami, G. Poggi, D. Sanderson, M. B. Tsang, H. M. Xu, D. E. Fields, K. Kwiatkowski, R. Planeta, V. E. Viola, Jr., S. J. Yennello, and S. Pratt, Phys. Rev. C **43**, R2474 (1991).
[3] A. Elmaani, N. N. Ajitanand, J. M. Alexander, R. Lacey, S. Kox, E. Liatard, F. Merchez, T. Motobayashi, B. Noren, C. Perrin, D. Rebreyend, Tsan Ung Chan, G. Auger, and S. Groult, Phys. Rev. C **43**, R2474 (1991).
[4] D. Goujdami, F. Guilbault, C. Lebrun, D. Ardouin, H. Dabrowski, S. Pratt, P. Lautridou, R. Boisgard, J. Quebert, and A. Peghaire, Z. Phys. A **339**, 293 (1991).
[5] W. G. Gong, C. K. Gelbke, W. Bauer, N. Carlin, R. T. de Souza, Y. D. Kim, W. G. Lynch, T. Murakami, G. Poggi, D. P. Sanderson, M. B. Tsang, H. M. Xu, D. E. Fields, K. Kwiatkowski, R. Planeta, V. E. Viola, Jr., S. J. Yennello, and S. Pratt, Phys. Rev. C **43**, 1804 (1991).
[6] H. Machner, M. Palarczyk, H. W. Wilschut, M. Nolte, and E. E. Koldenhof, Phys. Lett. B **280**, 16 (1992).
[7] D. H. Boal and J. C. Shillcock, Phys. Rev. C **33**, 549 (1986).
[8] J. Pochodzalla, C. B. Chitwood, D. J. Fields, C. K. Gelbke, W. G. Lynch, M. B. Tsang, D. H. Boal, and J. C. Shillcock, Phys. Lett. B **174**, 36 (1986).
[9] J. Pochodzalla, C. K. Gelbke, W. G. Lynch, M. Maier, D. Ardouin, H. Delagrange, H. Doubre, C. Gregoire, A. Kyanowski, W. Mittig, A. Peghaire, J. Peter, F. Saint-Laurent, B. Zwieglinski, G. Bizard, F. Lefebvres, B. Tamain, J. Quebert, Y. P. Viyogi, W. A. Friedman, and D. H. Boal, Phys. Rev. C **35**, 1695 (1987).
[10] Z. Chen, C. K. Gelbke, W. G. Gong, Y. D. Kim, W. G. Lynch, M. R. Maier, J. Pochodzalla, M. B. Tsang, F. Saint-Laurent, D. Ardouin, H. Delagrange, H. Doubre, J. Kasagi, A. Kyanowski, A. Peghaire, J. Peter, E. Rosato, G. Bizard, F. Lefebvres, B. Tamain, J. Quebert, and Y. P. Viyogi, Phys. Rev. C **36**, 2297 (1987).
[11] P. A. DeYoung, C. J. Gelderloos, D. Kortering, J. Sarafa, K. Zienert, M. S. Gordon, B. J. Fineman, G. P. Gilfoyle, X. Lu, R. L. McGrath, D. M. de Castro Rizzo, J. M. Alexander, G. Auger, S. Kox, L. C. Vaz, C. Beck, D. J. Henderson, D. G. Kovar, and M. F. Vineyard, Phys. Rev. C **41**, R1885 (1990).
[12] M. S. Gordon, R. L. McGrath, J. M. Alexander, P. A. DeYoung, Xiu qin Lu, D. M. deCastro Rizzo, and G. P. Gilfoyle, Phys. Rev. C **46**, R46 (1992).
[13] B. Jacobsson, B. Noren, A. Oskarsson, M. Westenius, M. Cronqvist, S. Mattson, M. Rydehell, O. Skeppstedt, J. C. Gondrand, B. Khelfaoui, S. Kox, F. Merchez, C. Perrin, D. Rebreyend, L. Westerberg, and S. Pratt, Phys. Rev. C **44**, R1238 (1991).
[14] S. E. Koonin, Phys. Lett. **70B**, 43 (1977).
[15] R. Lednicky and V. L. Lyuboshits, Yad. Fiz. **35**, 1316 (1982) [Sov. J. Nucl. Phys. **35**, 770 (1982)].
[16] S. Pratt and M. B. Tsang, Phys. Rev. C **36**, 2390 (1987).
[17] M. A. Bernstein, W. A. Friedman, and W. G. Lynch, Phys. Rev. C **29**, 132 (1984).
[18] M. A. Bernstein, W. A. Friedman, W. G. Lynch, C. B. Chitwood, D. J. Fields, C. K. Gelbke, M. B. Tsang, T. C. Awes, R. L. Ferguson, F. E. Obenshain, F. Plasil, R. L. Robinson, and G. R. Young, Phys. Rev. Lett. **54**, 402 (1985).
[19] M. Biyajima, Phys. Lett. **128B**, 24 (1983).
[20] M. A. Bernstein, W. A. Friedman, and W. G. Lynch, Phys. Rev. C **28**, 16 (1983).
[21] T. C. Awes, R. L. Ferguson, F. E. Obenshain, F. Plasil, G. R. Young, S. Pratt, Z. Chen, C. K. Gelbke, W. G. Lynch, J. Pochodzalla, and H. M. Xu, Phys. Rev. Lett. **61**, 2665 (1988).
[22] M. Korolija, D. Shapira, N. Cindro, J. Gomez del Campo, H. J. Kim, K. Teh, and J. Y. Shea, Phys. Rev. Lett. **67**, 572 (1991).
[23] D. Shapira, K. Teh, J. Blankenship, B. Burks, L. Foutch, H. J. Kim, M. Korolija, J. W. McConnell, M. Messick, R. Novotny, D. Rentsch, J. Shea, and J. P. Wieleczko, Nucl. Instrum. Methods A **301**, 76 (1991).
[24] K. Teh, D. Shapira, J. W. McConnell, H. J. Kim, and R. Novotny, IEEE Trans. Nucl. Sci. **35**, 272 (1988).
[25] G. I. Kopylov, Phys. Lett. **50B**, 472 (1974).
[26] W. A. Zajc, J. A. Bistirlich, R. R. Bossingham, H. R. Bowman, C. W. Clawson, K. M. Crowe, K. A. Frankel, J. G. Ingersoll, J. M. Kurch, C. J. Martoff, D. L. Murphy, J. O. Rasmussen, J. P. Sullivan, E. Yoo, O. Hashimoto, M. Koike, W. J. McDonald, J. P. Miller, and P. Truol, Phys. Rev. C **29**, 2173 (1984).
[27] F. Zarbakhsh, A. L. Sagle, F. Brochard, T. A. Mulera, V. Perez-Mendez, R. Talaga, I. Tanihata, J. B. Carroll, K. S. Ganezer, G. Igo, J. Oostens, D. Woodard, and R. Sutter, Phys. Rev. Lett. **46**, 1268 (1981).
[28] W. G. Lynch, C. B. Chitwood, M. B. Tsang, D. J. Fields, D. R. Klesch, C. K. Gelbke, G. R. Young, T. C. Awes, R. L. Ferguson, F. E. Obenshain, F. Plasil, R. L. Robinson, and A. D. Panagiotou, Phys. Rev. Lett. **51**, 1850 (1983).
[29] M. A. Lisa, W. G. Gong, C. K. Gelbke, and W. G. Lynch, Phys. Rev. C **44**, 2865 (1991).
[30] J. Gomez del Campo and R. Stokstad, ORNL Report No. TM7295, 1981 (unpublished).